NJC

Accepted Manuscript

This is an *Accepted Manuscript*, which has been through the Royal Society of Chemistry peer review process and has been accepted for publication.

Accepted Manuscripts are published online shortly after acceptance, before technical editing, formatting and proof reading. Using this free service, authors can make their results available to the community, in citable form, before we publish the edited article. We will replace this *Accepted Manuscript* with the edited and formatted *Advance Article* as soon as it is available.

You can find more information about *Accepted Manuscripts* in the Information for Authors.

Please note that technical editing may introduce minor changes to the text and/or graphics, which may alter content. The journal's standard Terms & Conditions and the Ethical guidelines still apply. In no event shall the Royal Society of Chemistry be held responsible for any errors or omissions in this *Accepted Manuscript* or any consequences arising from the use of any information it contains.

ROYAL SOCIETY OF CHEMISTRY

www.rsc.org/njc

Optical properties of thiophene-containing liquid crystalline and hybrid liquid crystalline materials

Jerzy Romiszewski,[a] *Zita Puterová-Tokarová,*[*a,b]* *Jozef Mieczkowski*[a] *and Ewa Gorecka*[a]

Mesogenic and optical properties of thiophene-based stilbenes and azobenzenes were investigated. A new hybrid material built of AuNP coated with thiophene-containing ligand is presented.

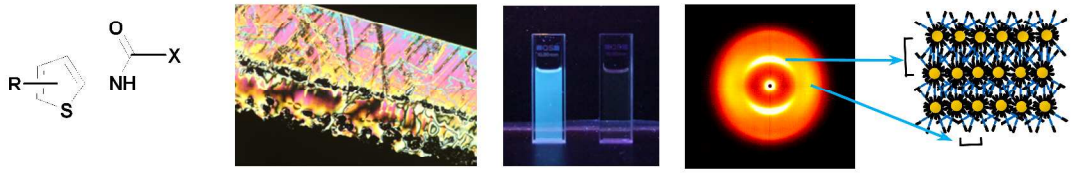

Cite this: DOI: 10.1039/c0xx00000x

www.rsc.org/xxxxxx

ARTICLE TYPE

Optical properties of thiophene-containing liquid crystalline and hybrid liquid crystalline materials

Jerzy Romiszewski,[a] Zita Puterová-Tokarová,*[a,b] Jozef Mieczkowski[a] and Ewa Gorecka[a]

Received (in XXX, XXX) XthXXXXXXXXX 20XX, Accepted Xth XXXXXXXXX 20XX

DOI: 10.1039/b000000x

We report new mesogens made of thiophene and stilbene moieties as main building blocks that exhibit nematic and/or smectic phases. The liquid crystalline properties in their thiophene/azobenzene analogues have been found to be strongly suppressed comparing to the thiophene/stilbene analogues. In twinned "bent-core" thiophene/azobenzene compound relatively strong fluorescence was found. A new hybrid material built of AuNP coated with thiophene-containing mesogenic ligand that forms smectic phase is shown. In solutions of thiophene-mesogen coated AuNP unusual decrease of ligand fluorescence decay rate was observed. Fluorescence lifetime increase is ascribed to two–point anchoring of ligand molecule resulting in molecule orientation tangential to AuNP surface. UV-Visible absorption and fluorescence data of all synthesised compounds are presented.

Introduction

Conjugated materials have received much attention as they offer new possibilities for devices combining desired optical, electrical and mechanical properties. Thiophenes and their functional derivates are among the variety of heterocyclic compounds used as key structural units in optoelectronic devices[1] such as field-effect transistors (OFETs)[2,3], organic-light emitting diodes (OLEDs)[4,5], photovoltaic cells[6] and chemosensors.[1,7] In fact, performance of such functional material is strongly dependent on its molecular structure and organization. Major efforts are presently being made in utilizing the liquid-crystalline (LC) state to organize π-conjugated semiconducting organic molecules in such way that high charge carrier mobilities can be achieved. As attractive as thiophene-containing materials are for their physical properties their synthesis is often challenging.[7] Alternating π-conjugated thiophene units with azobenzene and stilbene moieties can be used for changing and enhancing compounds optical and/or conducting properties as well as for introducing light-responsive properties. Azobenzene groups undergo a rapid *cis-trans* reversible isomerization by photoirradiation.[8,9] Therefore, azobenzenes are typically used as a photochromic switching elements for example in holographic recording devices[10] and for image storing applications.[11] Stilbenes also belong to systems that show reversible photoinduced *cis-trans* isomerization[12], exhibit strong blue fluorescence[13] and as pro-mesogenic entities in host thiophene-containing structures can introduce mesomorphic properties.[14] The optical anisotropy of such LC systems allows the generation of polarized light in OLEDs and polarized fluorescence which is of interest for security labels.[14-18] Advantage of both, azobenzene and stilbene elements, is their acceptable synthetic accessibility requiring only straightforward purification steps.[19,20] Their insertion into thiophene-based materials can lead to formation of a variety of mesomorphic structures with possible application for new types of optoelectronic devices. These discoveries have prompted our continuous research on development of novel mesogenic compounds with 2-aminothiophene core as main structural feature containing stilbene or azobenzene moiety. Along with investigations on mesogenic properties of target thiophene/stilbene and thiophene/azobenzene compounds the recent introduction of aminothiophene core helped us further to develop a mesogenic thiol-ended ligand for functionalization of gold nanoparticles (AuNPs). Recently much interest is being placed in the use of liquid crystals (LCs) for inducing controlled and eventually stimuli-responsive self-assembly of AuNPs[21-23] as well as for combining desired properties exhibited by both substrates that could result in new unique materials.[24-26] Functionalized AuNPs are key materials in nanochemistry and nanomaterial science with numerous applications ranging from opto-electronics[27], catalysis[28], to energy conversion devices.[29] Particle size and interparticle distance dependences of optical properties[30-32] in resulting AuNPs based materials make them a very promising building block that nevertheless requires appropriate method for controlled assembling.

We describe, herein, the synthesis, liquid-crystalline, optical behaviour and supramolecular organization in a novel type of hybrid AuNP grafted with amidothiophene-based soft layer (Fig. 1). The mesogenic and optical properties in thiophene/stilbene (Fig. 2) and thiophene/azobenzene compounds (Fig. 3) are investigated and compared, if possible. Preparation of substituted 2-aminothiophene core as a main element in the structure of all designed compounds was carried out by the Gewald reaction.[33] The availability of reagents and the mild reaction conditions all contribute to the versatility of this reaction, where by choosing a suitable substrates the structure of the final thiophene-containing material is precisely predicted.[14, 33]

Experimental

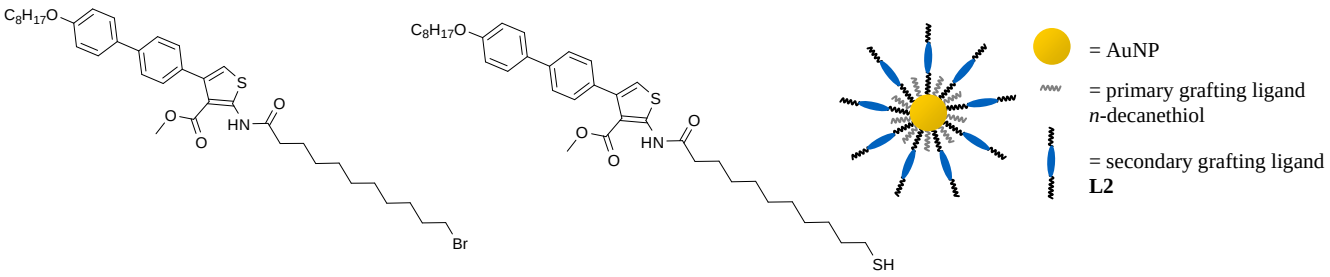

L1 **L2** **Au@L2**

Fig. 1 Molecular structures of ligand used as secondary grafting layer **L2** and its brominated precursor **L1**. Schematic structure of grafted nanoparticle **Au@L2**.

Synthesis of all presented compounds is described in the ESI† (Schemes S1 and S2). Gold NPs were synthesized according to the Brust method, using *n*-decanethiol to passivate the metal surface. The diameter of the metal particle core was determined from the small angle X-ray scattering of NPs in toluene solution. In the next step, part of the *n*-alkylthiol molecules were exchanged for the mesogenic molecules of compound **L2** (Fig. 1) by Murray reaction. The efficiency of the ligand exchange reaction was unambiguously confirmed by ^{1}H NMR spectra: broadening of signals coming from ligands covalently attached to the metal surface was observed. No traces of free ligands were found. Identification of the liquid crystalline phases was based on the type of texture exhibited by the compound. The textures were observed with a polarizing optical microscope (POM) Zeiss Axio Imager A2m equipped with a Linkam hot stage. The identification was confirmed by X-ray studies carried out on a Bruker GADDS system equipped with a VANTEC 2000 area detector and a hot stage controlled with a Linkam controller and on a BrukerNanostar equipped with a Vantec 2000 detector. CuKα radiation was used. Phase transition temperatures, enthalpies and melting points were determined by differential scanning calorimetry measurements on a TA Instruments DSC Q 200 calorimeter. In case that DSC measurement was inconclusive (no clear transition signal) or impossible (sample degradation accompanying heating) transition temperatures were determined by POM observation. Absorption spectra were recorded using a Shimadzu UV-3100 PC spectrometer for solutions of appropriate compounds in dichloromethane ($c \sim 5\times10^{-5}$ mol.dm^{-3}). Fluorescence measurements were performed for dilute solutions in dichloromethane using FluoroLog HORIBA JobinYvon spectrometer equipped with a TBX-04 PMT detector. Fluorescence lifetimes were calculated from fluorescence decay curves obtained by time-correlated single-photon counting method using the same FluoroLog HORIBA JobinYvon instrument with NanoLED excitation source.

Synthesis

In our study we have synthesized three series of compounds: *series A* – stilbene containing thiophenes **M1-M5** (Fig. 2); *series B* – azobenzene containing thiophenes **M6-M9** (Fig. 3) and *series C* – thiol-ended ligand **L2**, which was used for the preparation of gold nanoparticles **Au@L2**, and its bromo-

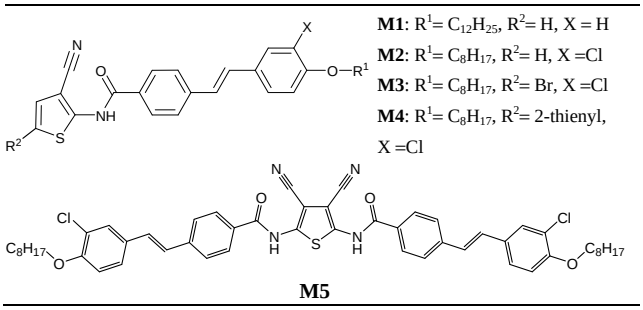

Fig. 2 Chemical structures of studied stilbene-containing thiophenes.

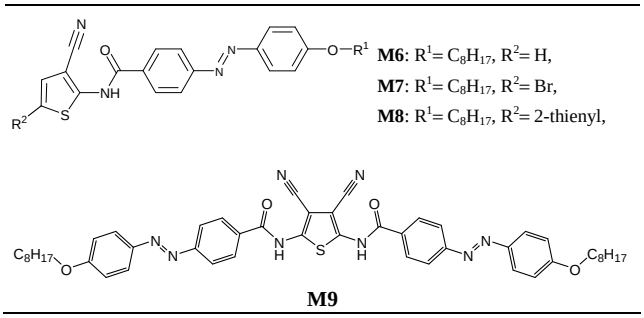

Fig. 3 Chemical structures of studied azobenzene-containing thiophenes.

substituted precursor **L1** (Fig. 1). The synthesis of **M1-M5** required preparation of stilbene fragment[20] terminated by long alkyloxy tail (C12, C8) and for compounds **M6-M9** substituted azobenzene with incorporated octyloxy chain was prepared in advance.[19] The 2-aminothiophene-3-carbonitrile as a main part of central core in compounds **M1**, **M2** and **M6** was synthesized utilizing the fourth version of the Gewald reaction.[34] Under standard reaction conditions using *N*-bromosuccinimide the corresponding 5-bromo-substituted derivatives **M3** and **M7** were formed.[35] New stilbene-containing bithiophene **M4** and its azobenzene homologue **M8** were synthesised employing palladium-catalysed coupling reactions.[36] 2,5-Diamino-thiophene-3,4-dicarbonitrile as a core unit in **M5** and **M9** was obtainable from tetracyanoethylene according to Middleton.[37] The central unit in **L1** and **L2**, the biphenyl-substituted-2-aminothiophene, was formed *via* modified Gewald reaction sequence published by us recently.[14] Generally, the Gewald reaction provides broad synthetic potential in material chemistry in synthesis of thiophene-containing metamaterials[14] and optoelectronics.[33] The methylester group in a position next to amino group stabilizes 2-aminothiophene core and enables subsequent reaction steps coupled with amino group substitution. It has to be noticed that substituted 2-aminothiophenes are stable

only if the electron-withdrawing group is present in the position C-3 adjacent to the amino group in C-2 of five-membered ring.[33,34] Exchanging bromine in **L1** with thiol group in **L2** was conducted according to the pioneering work[38] with hexamethyldisilathiane (HMDT) as thiolating agent.

Passivated gold nanoclusters were obtained by Brust-Schiffrin method[39] using *n*-decanethiol. The particles with simple *n*-alkylthiol (~ 55 thiol molecules per metal particle) did not form any long-range structure.[40] The radius of gold core, ~ 1.0 ± 0.2 nm, was determined by small-angle X-ray scattering (SAXS) experiments for particles dissolved in toluene.[38,40] In a ligand-exchange Murray reaction[41] *n*-decanethiol molecules were then substituted by mesogenic thiophene-containing ligand **L2** with thiol group pending at long C-10 alkyl chain (Fig. 1). The rate of exchange depends strongly on the Murray reaction conditions[42], and thus the temperature and concentration of incoming ligand were chosen to ensure that ~ 50 % of exchange ligand ratio was obtained. This result indicates that between 25 and 40 mesogenic groups were attached to a single gold particle. It was found previously that the type of nanoparticle organization is not affected by the number of mesogenic pendants within the limits given above.[38] For the detailed synthesis and characterization of all compounds see ESI†.

Mesomorphic properties and X-ray structural studies

All of the obtained stilbene-containing compounds form liquid-crystalline phases. Mesomorphic behaviour of compounds **M1-M4** is typical for rod-like molecules, exhibiting nematic and smectic A phases with relatively high (above 150 °C) melting and clearing temperatures. Compound **M5** despite its bent-core shape forms non-polar smectic C phase at elevated temperatures (above 300 °C). Because of high temperatures and moderate stability of **M5** compound it was not possible to confirm liquid-crystalline behaviour by XRD or DSC and the phase determination relied on POM observations. Among azo-compounds only **M7** compound with bromine in C-5 position of thiophene ring showed mesomorphic properties; it exhibits monotropic nematic phase. For **L1** precursor no LC phase was observed, while for thiol **L2** monotropic smectic A phase was found. Mesomorphic properties; transition enthalpies and temperatures for all studied materials are summarized in Table 1.

Although all stilbene-containing compounds show mesomorphic properties, only **M3** and **M4** exhibit a relatively broad temperature range (ca. 20 °C) of LC phase. Stability range of LC phases increases with elongation of alkyl chain (from **M1** to **M4**) and also upon introduction of halogen atoms (**M2, M3**) or additional thiophene ring (**M4**). Unfortunately **M4** undergoes partial decomposition at clearing temperature. We assume, that due to the exchanging of C=C bond by N=N bond the liquid crystalline properties of azo-compounds **M6**, **M8**, **M9** are hindered.[43] The lateral chloro-substitution on the benzene ring acts as a supplier of π-electrons lowering the dipole moment of the molecule, causing the decrease of the melting point of rod-like and banana-shaped stilbene-containing mesogens[44-47]; whereas the dipole moment of *trans* azobenzenes is equal zero regardless of the substitution.[48-50] Compound **M7**, with bromo-substituent on thiophene ring, is the only azo-derivative among studied that shows mesomorphic properties; it forms a monotropic nematic phase 10 °C beneath the melting point.

Table 1. Mesogenic properties, phase-transition temperatures (in °C) and enthalpies (in parentheses, kJ·mol^{-1}), and layer thicknesses in smectic A phase (in Å).

Comp.	T/°C [ΔH/kJ·mol^{-1}]	Layer thickness in SmA phase [Å]
M1	Cr 181.6 [30.58] Iso 180 [*][a]SmA 178.78 [31.4] Cr	35.8
M2	Cr 158.6 [20.4] N 164.4 [0.1] Iso 163.7 [0.7] N 150.62 [22.82] Cr	-
M3	Cr 158.2 [29.1] N 167.8 [0.55] Iso 170.4 [1.11] N [29.6] Cr	-
M4	Cr 61.7 [19.9] SmA 188.0 [0.47] N 242.9 [0.15] Iso 235.2 [3.49] N[b]	33.7
M5	Cr 310 [*] SmC[c]	-
M6	no LC	-
M7	Cr 211.6 [34.8] Iso 201.9 [0.2] N 198.0 [27.0] Cr	-
M8	no LC	-
M9	no LC	-
L1	no LC	-
L2	Cr 75.7 [40.8] Iso 53.2 [0.5] SmA 31.9 [30.0] Cr	35.1

[a] detected only by optical and X-ray measurements, [*] no data available
[b] probably due to partial decomposition on heating only iso-nematic transition is clear in cooling cycle
[c] phase transition is accompanied by decomposition, transition temperature based on POM observation, [*] no data available

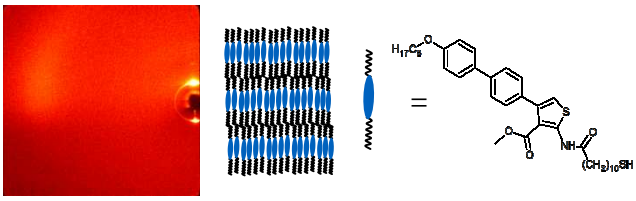

Fig. 4 XRD pattern of **L2** ligand in SmA phase just below clearing temperature, and the scheme showing arrangement of molecules in SmA phase and the molecular structure of **L2**.

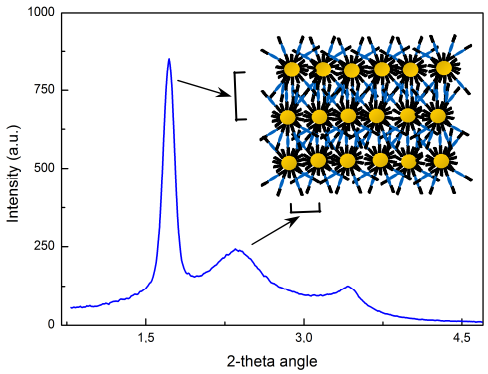

Fig. 5 Integrated X-ray pattern obtained for **Au@L2** at 140 °C together with schematic drawing showing arrangement of the NPs. The intense signal results from the layered structure with thickness d = 52.2 Å; weaker, diffuse signal (d = 37.3 Å) results from liquid-like in-plane order of gold particles inside the layer.

Table 2. UV-Visible absorption and fluorescence data for all prepared compounds.

Comp.	UV-Visible			Fluorescence		
	λ_{max} [nm]	ε [$dm^3 \cdot cm^{-1} mol^{-1}$]	E_g^{opt} [eV]	λ_{max} [nm]	τ[ns]	Relative amplitude [%]
M1	350.5	25200	3.11	451	0.16	97.4
					0.50	2.1
M2	349.5	40400	3.14	438	0.20	93.2
					0.13	6.5
M3	347.0	40500	3.10	438	0.40	98.7
					10.8	1.3
M4	359.0	23580	2.85	443	0.49	91.2
					0.28	8.4
M5	355.0	26200	2.92	516	1.4	67.6
					0.17	27.6
M6	369.5	27900	2.34	-	-	-
M7	371.0	27200	2.34	-	-	-
M8	374.5	5940	2.27	-	-	-
M9	365.5	17190	2.34	510	1.60	84.2
					0.72	12.0
L1	267.5	21100	2.79	392	0.17	92.3
					1.70	6.7
L2	268.0	29500	2.82	392	0.16	95.1
					1.50	3.4
Au@L2	267.5	-	-	371	0.17	48.6
					1.50	43.6
					8.70	7.8

Measurements taken in dichloromethane at room temperature, typical concentration $c = 5 \cdot 10^{-5}$ mol.dm^{-3}

The **Au@L2** system was designed with the aim of producing a gold nanoparticle-based LC with relatively simple coating layer that could be compatible for doping with M-series compounds or could be used as a dopant for these compounds.

Ligand **L2** forms a monotropic SmA phase with layer thickness ~ 35.1 Å which is close to the length of a fully stretched molecule (Fig. 4). Due to the presence of –SH terminal group (Fig. 1) it can be also introduced as a secondary ligand, by partial exchanging of primary alkyl ligand at the metal surface of AuNPs.

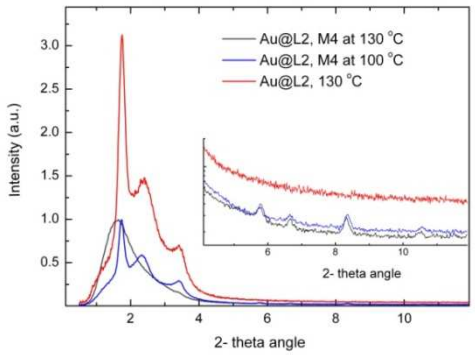

Fig. 6 Integrated XRD patterns for **Au@L2** and the composite of **Au@L2** with **M4** compound. In the inset is magnified region at higher angles, showing the signals from crystal structure of **M4**.

The gold nanoparticles coated with **L2** ligand show lamellar phase (Fig. 5). Long-range positional order for the structure formed by hybrid **Au@L2** was confirmed by X-ray studies; two sharp, commensurate XRD signals in a small angle region indicate the presence of a lamellar structure with the layer thickness d = 52.2Å (Fig. 4) that is only weakly dependent on temperature. The measured layer periodicity for **Au@L2** system is much larger than observed for ligand **L2** in smectic phase. The mean distance between the gold particles inside the layers, calculated from position of diffuse signal, is 37.3 Å. Taking into account diameter of metal particles (~ 10 Å), molecular lengths of *n*-decanethiol and **L2** molecule, one can propose the model of the structure in which gold particles are arranged in the sublayers separated by organic sublayers. The organic sublayers are made of **L2** molecules that are collected below and above metal cores. Ligands attached to the particles from neighbouring metal sublayers intertwine with one another, whereas *n*-alkyl ligands are evenly distributed around gold centres and determine the distance between gold particles in the sublayer. Lack of measurable birefringence of the structure shows that there is no orientational order of **L2** ligands in the organic sublayer. Heating of the **Au@L2** above 160 °C causes decomposition; such decomposition prevents observation of isotropic melt.

Because melting temperatures of M-series compounds are close to decomposition temperature of **Au@L2** material composites were prepared by dissolving both **Au@L2** and **M4**

compound in appropriate solvent and slow evaporation of the solvent. The XRD measurements prove that only a limited amount of **M4** compound can be incorporated into **Au@L2** matrix and the rest of the M-compound precipitates in crystalline state. The X-ray pattern of mixture shows signals coming from the layer structure formed by NPs and a few sharp reflections (the signal at 3.4 deg overlaps with the peak of second harmonic of NPs smectic phase) coming from crystal structure of **M4** (Fig. 6). The layer thickness of composite is unchanged compared to pure **Au@L2** material but the in-plane distance between NPs slightly increased, which is probably due to the introduction of some of the dopant molecules and/or secondary grafting molecules (**L2**) between the AuNPs within the layer. The composite melts at lower temperature (~ 130 °C) however, even in the melt the excess of **M4** phase stays separated. We believe that slight modifications of both ligand (**L2**) and dopant molecules should improve stability of composites, paving the way for light responsible AuNP LC`s.

Optical properties: UV-Visible absorption and Fluorescence

For all studied compounds, ligands as well as for **Au@L2** gold particles, UV-Visible absorption spectra, fluorescence spectra and fluorescence lifetime were measured. Results are summarized in Table 2.

Stilbene derivatives (Fig. 7) **M1-M5** exhibit single optical absorption band around 350 nm and fluorescence band around 445 nm. The twinning of molecular structure (compound **M5**) does not change much optical absorption spectra but introduces a considerable redshift in fluorescence spectrum, emission is observed at 516 nm. Azo-compounds **M6-M9** are characterised by the main absorption band at 370 nm (π-π* transition in *trans* form) with small tail without very clearly differentiated peaks at longer wavelength. From data fit one can deduce position of the second absorption band at around 465 nm. Twinning of the structure (compound **M9**) leads only to a very slight blue-shift of absorption to 366 nm (Fig. 8). Stilbene compounds **M1-M4** are characterized by fluorescence in blue region with fast, single exponential decay (with lifetime below 500 ps) whereas **M5** exhibits more complex, multiexponential decay, its major component having lifetime ~ 1.5 ns. For azo materials **M6-M8**, fluorescence is strongly quenched. Contrary to this typical behaviour, for the material **M9** with two azo- units, relatively strong fluorescence at 510 nm was observed with decay time of 1.6 ns. The Uv-Visible absorption measurements performed for **M6-M8** (Fig. 9) during, or shortly after irradiation with Uv light (350-380 nm) showed typical spectrum changes related to photo-induced *cis*-isomerisation, i.e. a sharp decrease of intensity of absorption band due to π-π* transition in *trans* form at 370 nm, occurrence of new absorption band with maximum at 322 nm due to π-π* transition in *cis*-form and increased intensity of absorption band due to n-π* transition in *cis*-form at 442 nm. For *bis*-azo compound **M9**, even after longer Uv irradiation absorption at 370 nm remains but also increases in absorptions at ca. 460 and 300 nm, as typical for *trans-cis* transition, are observed. Still irradiation of **M9** with visible light reproduces original shape of absorption spectrum (Fig. 10).

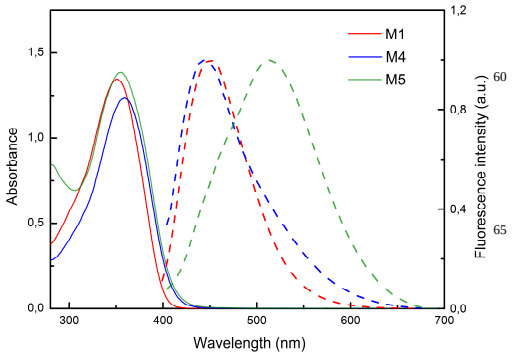

Fig. 7 UV-Visible absorption (solid line) and fluorescence (dashed line) spectra for **M1-M5** compounds.

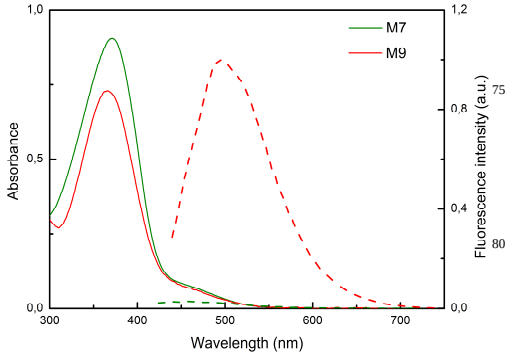

Fig. 8 UV-Visible absorption (solid line) and fluorescence (dashed line) spectra of **M7**.

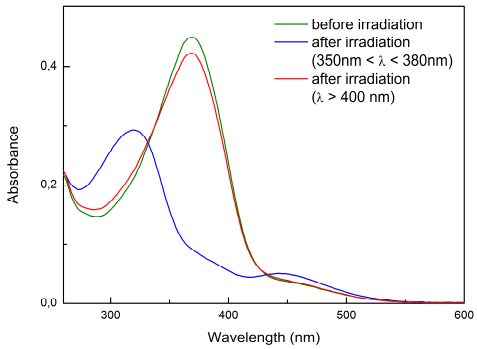

Fig. 9 UV-Visible absorption spectra of **M6** before and after UV irradiation.

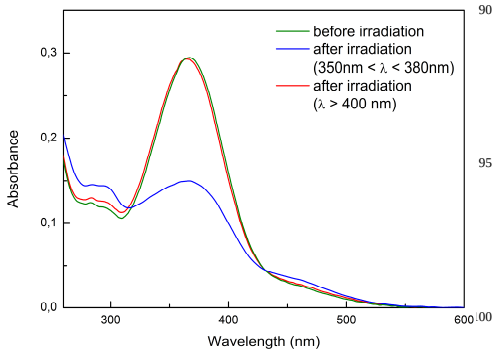

Fig.10 UV-Visible absorption spectra of **M9** before and after UV irradiation.

The absorption band of **L1** and **L2** compounds due to coupling of biphenyl and thiophene moieties is red shifted with respect to components and exhibit maximum absorption at 268 nm and fluorescence at 392 nm with very short decay time of ca. 170 ps. Also ligand **L2** attached to gold particles shows fluorescence with a slight blue shift (371 nm). This is rather unusual observation since in most cases proximity of metal surface strongly affects fluorescence of attached ligand[51,52], resulting in fluorescence quenching and shortening of fluorescence lifetime. Contrary to this general behaviour, for ligand **L2** attached to the gold nanoparticles (**Au@L2**), fluorescence decay time becomes significantly longer than for free ligand (Fig. 11), due to appearance of a new decay term with lifetime of 1.5 ns.[38] Fluorescence lifetime increase in the proximity of metal surface was theoretically predicted already over 10 years ago[51,52] but to our best knowledge such effect was reported only once so far and for a fluorophore structurally constraint to align parallel to AuNP surface.[53]

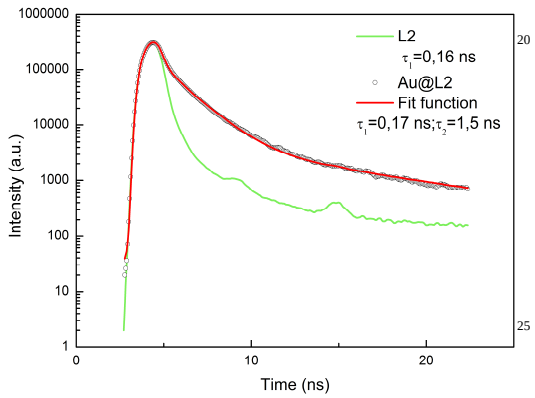

Fig. 11 Fluorescence decay for free ligand **L2** and nanoparticle **Au@L2**. Bumps on **L2** fluorescence decay signal are experimental artefacts due to characteristic time of excitation signal.

Results and discussion

2-Aminothiophene ring as a main structural element was introduced into two series of rod-like and bent-core compounds differing in the structure of the side fragment – stilbene **M1**-**M5** *vs.* azobenzene **M6**-**M9**. Their mesogenic and optical properties were investigated and compared, if possible. Ordered structures are promoted by planarity and aromatic character of stilbene unit in the mesogenic core. Previously we have reported investigations on stilbene-containing thiophenes possessing mesogenic properties with high transition temperatures.[14] In order to lower the clearing temperatures, herein we have prepared stilbene fragment with chloro-substituent adjacent to octyloxy chain on benzene ring (**M2**-**M5**). Incorporation of lateral halogen substituent on benzene ring of rod-like and banana-shaped mesogens containing stilbenes is a common procedure to decrease their melting points.[44-47] Nevertheless high stability of crystalline phase in **M1**-**M5** results in relatively narrow range of LC phases. Higher stability of LC phases formed by **M3** and **M4** may be rationalised by higher number of halogen atoms (2 versus 1 in other compounds in this series – **M1**-**M4**) and therefore larger dipole moment for **M3** as well as increased length of aromatic core (by introduction of second thienyl unit) in **M4**. The same extension of aromatic core leads to very high melting temperature in **M5**. Although both azobenzene and stilbene unit are often used as promesogenic entities[54,55] in **M6**-**M9** – that are close structural azo-analogues of compounds **M1**-**M5**, only **M7** displays mesogenic phase. This behaviour is in line with general tendency for lowering of nematic-isotropic phase transition temperature upon exchanging C=C by N=N unit in R^1-Ph-X=X-Ph-R^2 compounds (X = C, N).[43] Generally, the influence of halo-substitution on mesophase stability is ambiguous and probably introduction of halogen would have only minor impact on the formation of mesophases in **M6**, **M8** and **M9**.[43,56-58] Still the introduction of of bromine to α-position of thiophene ring in **M7** leads to the formation of monotropic nematic phase at relatively high temperature (200 °C). Therefore the influence of lateral halogen substituent in azobenzenes cannot be completely neglected and could become a topic of further scrutiny.

Stilbene derivatives exhibit, as typical for this group of materials, optical properties with single strong absorption band around 350 nm and fluorescence band around 440 nm. For **M5** compound the fluorescence band shifts to 516 nm and fluorescence decay time increases, due to the extending of mesogenic core by additional aromatic rings. Single azo-group derivatives **M6**-**M8** are not fluorescent, such behaviour is typical for azo compounds.[43] These materials show also typical absorbance spectrum consisting of high intensity absorption band around 370 nm due to π-π* transition in *trans*-form and small intensity tail at longer wavelengths. Absorption tail is mostly due to the weak n-π* transition for *trans*-form. Quite unusual is relatively strong fluorescence observed for azo-compound **M9**. Changes in absorption spectrum upon Uv irradiation indicate that only part of azo groups can undergo *cis-trans* isomerisation whereas the rest remains in *trans* form.

New liquid crystalline hybrid material was obtained by exchanging part of *n*-decanethiol primary grafting layer at gold nanoparticle by mesogenic thiophene-biphenyl compound (**L2**). To the best of our knowledge, aminothiophene chemistry was not applied for the preparation of such nanomaterials so far. Advantage of this thiophene-based ligand besides acting as secondary grafting for gold nanoparticle, is its ability to form smectic A mesophase with relatively low transition temperature (52.2 °C, Table 1). The gold nanoparticle with thick deformable organic layer formed lamellar structure build of metal particle rich sublayers divided by organic sublayers however with no intrinsic orientational ordering of ligands. The unusual elongation of fluorescence decay time of **Au@L2** solutions in comparison to solutions of free ligand is rather surprising as for radial distributed ligand a contrary effect is expected.[51,52] On the other hand for ligand aligned parallel to the metal surface, as predicted theoretically, fluorescence decay time becomes longer than for ligands aligned perpendicular to gold surface.[51,52] Such effect was observed for dithiol ligand (4-acetamido-4`-maleimidylstilbene-2,2`-dithiol) which parallel alignment to the AuNP surface was enforced by double point anchoring to the surface.[53] Although **L2** ligand contains one thiol group in its structure two point anchoring to AuNP surface is also possible. It is known that thiophene derivatives exhibit ability for binding to gold surface via sulfur atom, forming self-assembled monolayers on planar surfaces and partially coating Au nanoparticles[59] thus one can expect that at least part of **L2** molecules is bound to AuNP

surface both *via* thiol group and sulfur atom of thiophene group. **Au@L2** fluorescence decay can be fairly well described by a two exponential model with almost equal share of fast (τ = 0.17 ns) and slow (τ = 1.5 ns) decay. As the time constant of the fast decay is almost the same as that measured for free ligand molecules, one can propose a model in which there are two types of **L2** particles on AuNP surface: 1) only thiol bound, on average radially oriented and exhibiting fluorescence decay rate close to that of free **L2**; 2) bound by thiol and thiophene and thus oriented inclined towards AuNP surface with a slower fluorescence decay. Such an arrangement in which there is no clearly preferenced orientation of ligand particles would also imply none or very low birefringence. This is in agreement with our observation in pure, planarly oriented (layers perpendicular to the surface), hybrid nanoparticle LC state. Concluding a plausible explanation of observed elongation of fluorescence lifetime is provided by the assumption that at least part of ligand particles in **Au@L2** is bound *via* thiol as well as thiophene group resulting in rather tangential than planar average orientation of ligand molecules. Further research to validate this assumption is under way.

Conclusions

The mesomorphic and optical properties of several rod-like and bent-core compounds derived from 2-aminothiophene with stilbene and azobenzene moiety have been investigated. The mesophases exhibited by thiophene/stilbene compounds have been characterized as the nematic and the smectic A phase, typical for rod-like and bent-core molecules. The mesogenic behaviour in their thiophene/azobenzene analogues was found to be strongly supressed, except of only one derivative containing halogen on thiophene ring exhibiting monotropic nematic phase with low stability. Exchange of C=C bond to N=N seems to play the main role in hindering mesophase formation in azobenzene compounds in comparison with mesogenic stilbene relatives. At present, some contribution of halo-substitution could be recognized. Single optical absorption bands in thiophene/stilbenes and thiophene/azobenzenes were observed in near UV region. Twinning of the molecule does not change optical absorption for stilbene-like thiophenes and in thiophenes with azobenzene unit leads only to a very slight blue-shift. While stilbene compounds are characterized by fluorescence in blue region, the fluorescence in azobenzene/thiophenes is quenched, except for material with two azobenzene units exhibiting relatively strong fluorescence.

The gold nanoparticle grafted with aminothiophene-based ligand was characterized to form lamellar phase with periodicity only weakly dependent on temperature. Ligand itself was found to form SmA phase at relatively low-temperatures. The absorption and fluorescence of free ligand is red shifted with respect to the ligand attached to gold surface with slight blue shift. Unique elongation of fluorescence decay time of AuNPs comparing to free ligand was observed for the first time, when thiophene grafting is used.

Notes and references

[*a]*Department of Chemistry, Warsaw University, Pasteura 1, 02-093 Warsaw, Poland. Tel:+4822 8220211; E-mail: z.puterova@chem.uw.edu.pl

[b]*Department of Chemistry, University of SS Cyril and Methodius, Nám. J. Herdu 2, 917-01 Trnava, Slovakia. Fax:+421335921403; Tel:+421335921408; E-mail: zita.tokarova@ucm.sk*

† Electronic Supplementary Information (ESI) available: Synthesis, experimental details of methods used for synthesis, characterization of all obtained compounds, figures of UV-Vis absorption and fluorescence spectra for all compounds. See DOI: 10.1039/b000000x/

Acknowledgements

Presented work was supported by FNP Project TEAM/2010-5/4: "*Self-assembly of functionalized inorganic-organic liquid crystalline hybrids for multifunctional nanomaterials*."

Support of the Foundation for Polish Science under MPD programme cofinanced by the EU European Regional Development Fund is greatly acknowledged.

The support of the Ministry of Education of the Slovak Republic – VEGA 1/0073/13 is also acknowledged.

References

1 A. Mishra, Ch.-Q. Ma, P. Bäuerle, *Chem. Rev*., 2009, **109**, 1141

2 I. McCullogh, M. Heeney, C. Bailey, K. Genevicius, I. MacDonald, M. Shkunov, D. Sparrowe, S. Tierney, R. Wagner, W. Zhang, M. L. Chabinyc, R. J. Kline, M. D. Mcgehee, M. F. Toney, *Nat. Mater*., 2006, **5**, 328

3 F. Garnier, G. Horowitz, X. Peng, D. Fichou, *Adv. Mater*., 1990, **2**, 592

4 J. H. Seo, E. B. Namdas, A. Gutacer, A, J. Heeger, G. C. Bazan, *Adv. Funct. Mater*., 2011, **21**, 3667

5 F. Geiger, M. Stoldt, H. Schweizer, P. Baüerle, E. Umbach, *Adv. Mater*., 1993, **5**, 922

6 H. Bronstein, Z. Chen, R. S. Ashraf, W. Zhang, J. Du, J. R. Durrant, P. S. Tuladhar, K. Song, S. E. Watkins, Y. Geerts, M. M. Wienk, R. A. J. Janssen, T. Anthopoulos, H. Sirringhaus, M. Heeneynad, I. McCullogh, *J. Am. Chem. Soc*., 2011, **133**, 3272

7 S. Dufresne, M. Bourgeaux, W. G. Skene, *J. Mater. Chem*., 2007, **17**, 1166

8 H. M. Dhammika Bandara, S. C. Burdette, *Chem. Soc. Rev.*, 2012, **41**, 1809

9 N. Tamai, H. Miyasaka, *Chem. Rev*., 2000, **100**, 1875

10 P. Varhegyi, A. Kerekes, S. Sajti, F. Ujhelyi, P. Koppa, G. Szarvas, E. Lorincz, *Appl. Phys. B: Laser Opt*., 2003, **76**, 397

11 T. Ikeda, T. Ube, *Mater. Today*, 2011, **14**, 480

12 P. Tegeder, *J. Phys.: Condens. Matter*, 2012, **24**, 394001

13 J. Saltiel, Y.-P. Sun, *Photochromism, Molecules and Systems*; H. Dürr, H. Bounas-Laurent, Eds.; Elsevier: Amsterdam 2003

14 Z. Puterová, J. Romiszewski, J. Mieczkowski, E. Gorecka, *Tetrahedron*, 2012, **68**, 8172

15 Tschierske, C., *J. Mater. Chem.*, 2008, **18**, 2869

16 M. Funahashi, J. Hanna, *Adv. Mater.*, 2005, **17**, 594

17 A. J. J. M. van Breemen, P. T. Herwig, C. H. T. Chlon, J. Sweelssen, H. F. M. Schoo, S. Setayesh, W. M. Hardeman,C. A. Martin, D. M. de Leuw, J. J. P. Valnton, C. W. M. Bastiaansen, D. J. Broer, A. R. Popa-Merticaru, S. C. J. Meskers, *J. Am. Chem. Soc*., 2006, **128**, 2336

18 T. Yasuda, H. Ooi, J. Morita, Y. Akama, K. Minoura, M. Funahashi, T. Shimomura, T. Kato, *Adv. Funct. Mater*., 2009, **62**, 411

19 F. Vera, R. M. Tejedor, P. Romero, J. Barberá, M. B. Ros, J. L. Serrano, T. Sierra, *Angew. Chem. Int. Ed.*, 2007, **46**, 1873

20 K. Gomola, L. Guo, S. Dhara, Y. Shimbo, E. Gorecka, D. Pociecha, J. Mieczkowski, H. J. Takezoe, *J. Mater. Chem.*, 2009, **19**, 4240

21 M. Draper, I. M. Saez, S. J. Cowling, P. Gai, B. Heinrich, B. Donnio, D. Guillon, J. W. Goodby, *Adv. Funct. Mater*. 2011, **21**, 1260

22 M. M. Wojcik, M. Gora, J. Mieczkowski, J. Romiszewski, E. Gorecka, D. Pociecha, *Soft Matter*, 2011, **7**, 10561

23 J. Milette, S. J. Cowling, V. Toader, C. Lavigne, I. M. Saez, R. B. Lennox, J. W. Goodby, L. Raven, *Soft Matter*, 2012, **8**, 173

24 M. Wojcik, M. Kolpaczynska, D. Pociecha, J. Mieczkowski, E. Gorecka, *Soft Matter*, 2010, **6**, 5397

25 J. W. Goodby, I. M. Saez, S. J. Cowling, V. Görtz, M. Draper, A. W. Hall, S. Sia, G. Cosquer, S.-E. Lee, E. P. Rayners, *Angew. Chem. Int. Ed.*, 2008, **47**, 2754

26 J. Pérez-Juste, I. Pastoriza-Santos, L. M. Liz-Marźan, P. Mulvaney, *Coord. Chem. Rev*., 2005, **249**, 1870

27 R. Schlögl, S. B. A. Hamid, *Angew. Chem. Int. Ed.*, 2004, **43**, 1628

28 S. E. Lohse, C. J. Murphy, *J. Am. Chem. Soc*., 2012, **134**, 15607

29 R. Sardar, A. M. Funston, P. Mulvaney, R. W. Murray, *Langmuir*, 2009, **25**, 13840

30 S. Eustis, M. A. Sayed, *Chem. Soc. Rev*. 2006, **35**, 209

31 A. Rizzo, C. Nobile, M. Mazzeo. M. De Giorgi, A. Fiore, L. Carbone, R. Cingolani, L. Manna, G. Gigli, *ACS Nano*, 2009, **3**, 1506

32 D. V. Talapin, J.-S. Lee, M. V. Kovalenko, E. V. Shevchenko, *Chem. Rev*., 2010, **110**, 389

33 Z. Puterová, A. Krutošíková, D. Végh, *ARKIVOC*, 2010, **1**, 209.

34 K. Gewald, *Chem. Ber.*, 1965, **98**, 3571

35 R. Wu, J. S. Schumm, D. L. Pearson, J. M. Tour, *J. Org. Chem*. 1996, **61**, 6906

36 E.V. Verbitskiy, E. M. Cheprakova, P. A. Slepukhin, M. I. Kodess, M. A. Ezhikov, M. G. Pervova, G. L. Rusinov, O. N. Chupakhin, V. N. Charushin, *Tetrahedron*, 2012, **68**, 5445

37 W. J. Middleton, *Org. Synth.*, 1963, **coll. Vol. 4**, 243

38 M. Wojcik, W. Lewandowski, J. Matraszek, J. Mieczkowski, J. Borysiuk, D. Pociecha, E. Gorecka, *Angew. Chem. Int. Ed.*, 2009, **48**, 5167

39 M. Brust, M.Walker, D. Bethell, D. J. Schiffrin, *J. Chem. Soc. Chem. Commun*., 1994, 801

40 J. M. Wolska, D. Pociecha, J. Mieczkowski, E. Gorecka, *Soft Matter*, 2013, **9**, 3005

41 A. C. Templeton, M. J. Hostetler, C. T. Kraft, R. W. Murray, *J. Am. Chem. Soc*., 1998, **120**, 1906

42 A. Dass, K. Holt, J. F. Parker, S. W. Feldberg, R. W. Murray, *J. Phys. Chem. C*, 2008, **112**, 20276

43 T. Tsuji, H. Takeuchi, T. Egawa, S. Konaka, *J. Am. Chem. Soc.*, 2001, **123**, 6381

44 P. Gisse, P. Cluzeau, V. Ravaine, H. T. Nguygen, *Liq. Cryst*., 2002, **29**, 91

45 W. Weissflog, H. Nadasi, U. Dunemann, G. Pelzl, S. Diele, A. Eremin, H. Kresse, *J. Mater. Chem*., 2002, **12**, 1316

46 H. Nadasi, W. Weissflog, A. Eremin, G.Pelzl, S. Diele, B. Das, S. Grande, *J. Mater. Chem*., 2002, **12**, 1316

47 P. Pyc, J. Meczkowski, D. Pociecha, E. Gorecka, B. Donnio, D. Guillon, *J. Mater. Chem*., 2004, **14**, 2374

48 M. Ucar, K. Polat, A. O. Solak, M. Toy, M. L. Aksu, *Dyes Pigm.*, 2010, **87**, 55.

49 G. S. Hartley, *Nature*, 1937, **140**, 281.

50 D. Canakci, M. Tuncel, H. Mart, S. Serin, *Polym. Int*., 2007, **56**, 1537

51 W. L. Barnes, *J. Mod. Optic.*, 1998, **45**, 661

52 H. Chew, *J. Chem. Phys.*, 1987, **87**, 1355

53 F. E. Hernandez, S. Yu, M. Garcia, A. D. Campiglia, *J. Phys. Chem. B*, 2005, **109**, 9499

54 L. Rozes, C. Noel, I. Campistron, M. Thomas, D. Reyx, F. Kajzar, *Macromol. Chem. Phys.*, 1998, **199**, 2553

55 E. Wolarz, Th. Fischer, J. Stumpe, *Thin Solid Films*, 2003, **424**, 179

56 B. C. Chauhan, A. A. Doshi, A. V. Doshi, *Mol. Cryst. Liq. Cryst*., 2013, 570, 84

57 M. E. Neubert, L. T. Carlino, R. D'Sidocky, D. L. Fishel, In *Liquid Crystals and Ordered Fluids*; Johnson J. F., Porter R. S., Eds.; Plenum Press: New York, 1973; Vol. 2, p 293

58 L. E. Knaak, H. M. Rosenberg, M. P. Serve´, *Mol. Cryst. Liq. Cryst*, 1972, **17**, 171

59 F. Terzi, R. Seeber, L. Pigani, Ch. Zanardi, L. Pasquali, S. Nannarone, M. Fabrizio, S. Daolio, *J. Phys. Chem. B*, 2005, **109**, 19397